International Journal of Remote Sensing
Vol. 32, No. 24, 20 December 2011, 9007–9031

Taylor & Francis
Taylor & Francis Group

Hyperspectral remote sensing for estimating aboveground biomass and for exploring species richness patterns of grassland habitats

A. PSOMAS*†‡, M. KNEUBÜHLER‡, S. HUBER§, K. ITTEN‡ and N. E. ZIMMERMANN†

†Swiss Federal Research Institute WSL, Zuercherstrasse 111, 8903 Birmensdorf, Switzerland

‡Remote Sensing Laboratories (RSL), Department of Geography, University of Zürich, Winterthurerstrasse 190, 8057 Zürich, Switzerland

§Department of Geography and Geology, University of Copenhagen, Øster Voldgade 10, 1350 Copenhagen, Denmark

(*Received 16 September 2009; in final form 13 October 2010*)

Dry grassland sites are amongst the most species-rich habitats of central Europe and it is necessary to design effective management schemes for monitoring of their biomass production. This study explored the potential of hyperspectral remote sensing for mapping aboveground biomass in grassland habitats along a dry-mesic gradient, independent of a specific type or phenological period. Statistical models were developed between biomass samples and spectral reflectance collected with a field spectroradiometer, and it was further investigated to what degree the calibrated biomass models could be scaled to Hyperion data. Furthermore, biomass prediction was used as a surrogate for productivity for grassland habitats and the relationship between biomass and plant species richness was explored. Grassland samples were collected at four time steps during the growing season to capture normally occurring variation due to canopy growth stage and management factors. The relationships were investigated between biomass and (1) existing broad- and narrowband vegetation indices, (2) narrowband normalized difference vegetation index (NDVI) type indices, and (3) multiple linear regression (MLR) with individual spectral bands. Best models were obtained from the MLR and narrowband NDVI-type indices. Spectral regions related to plant water content were identified as the best estimators of biomass. Models calibrated with narrowband NDVI indices were best for up-scaling the field-developed models to the Hyperion scene. Furthermore, promising results were obtained from linking biomass estimations from the Hyperion scene with plant species richness of grassland habitats. Overall, it is concluded that ratio-based NDVI-type indices are less prone to scaling errors and thus offer higher potential for mapping grassland biomass using hyperspectral data from space-borne sensors.

1. Introduction

Grasslands belong to the earth's largest biomes and represent the most important source of livestock feeding. More important, however, is their contribution to ecological goods and services, and to the diversity and cultural history of rural and

*Corresponding author. Email: Achilleas.Psomas@wsl.ch

International Journal of Remote Sensing
ISSN 0143-1161 print/ISSN 1366-5901 online © 2011 Taylor & Francis
http://www.tandf.co.uk/journals
http://dx.doi.org/10.1080/01431161.2010.532172

agricultural landscapes. Grasslands are one of the major sources of biodiversity in Europe, where they cover 50% of the total cultivated area (Tueller 1998) and represent a promising opportunity to restore or conserve biodiversity in agricultural landscapes (Duelli and Obrist 2003). Productivity of these grasslands has a strong effect on both species competition and human management schemes, since highly productive grasslands are more prone to be converted to, or remain as, agricultural areas. Development of robust and timely biomass estimates is of critical importance for monitoring and designing effective management practices that optimize sustainability of these ecosystems and their goods and services over time.

Traditional methods for mapping grassland biomass involve direct measurements, which are time-consuming, expensive and require extensive field work. Furthermore, reliable estimates are restricted to local scales only, whereas ecologists and managers require estimates at the landscape scale. One of the major sources of information for the study of landscapes and for estimating biomass over large areas is remote sensing (Kumar *et al*. 2001, Wulder *et al*. 2004). Attempts to estimate biomass using broadband sensors with spatial resolutions of 30 m to 1 km have resulted in a wide range of accuracies and precision (Todd *et al.* 1998, Wylie *et al.* 2002, Kogan *et al.* 2004, Geerken *et al.* 2005, Dengsheng 2006). Even though averaging of spectral information over broad bandwidths can result in loss of critical information (Blackburn 1998), the quantity and spatial distribution of grassland biomass, in most of these studies, was estimated through the use of broadband vegetation indices (VIs).

Recently, hyperspectral sensors that acquire images in a large number of narrow spectral channels (over 40) have been developed (Van der Meer *et al.* 2001). Studies using hyperspectral data to estimate biomass have been carried out under controlled laboratory conditions (Mutanga and Skidmore 2004a, b) and in the field for yield estimation of agricultural crops such as wheat and corn (Osborne *et al.* 2002, Hansen and Schjoerring 2003, Zarco-Tejada *et al.* 2005, Xavier *et al.* 2006). A limited number of studies exist that have investigated the relationship between hyperspectral remote sensing and biomass production of mixed grassland ecosystems (Rahman and Gamon 2004, Mirik *et al.* 2005, Tarr *et al.* 2005, Beeri *et al.* 2007, Cho *et al.* 2007) and only a few exist (Filella *et al.* 2004, Geerken *et al.* 2005, Boschetti *et al.* 2007) that have extended such analyses over the growing season.

Furthermore, statistical relationships between biomass and spectral information have often been established between field spectrometer measurements and biomass (Thenkabail *et al.* 2000, Künnemeyer *et al.* 2001, Osborne *et al.* 2002, Filella *et al.* 2004, Mutanga and Skidmore 2004a, Shen *et al.* 2008), field spectrometer measurements resampled to match band definition of existing hyperspectral or broadband sensors and biomass (Hansen and Schjoerring 2003, Xavier *et al.* 2006) and between spectral reflectance extracted directly from hyperspectral sensors and concurrent field biomass sampling (Mirik *et al.* 2005, Zarco-Tejada *et al.* 2005, Kooistra *et al.* 2006). Only very few studies have attempted to up-scale field-developed statistical models to the sensor level (Zha *et al.* 2003, Anderson *et al.* 2004) and none, to our knowledge, have attempted to up-scale statistical models calibrated using observations collected over the span of the growing season.

A common characteristic of many of the above-mentioned studies is that they do not attempt to answer specific ecological questions using remote sensing-derived products. The relationship between productivity and species richness has been of long-standing interest to ecologists, because understanding the mechanisms driving this relationship can help us comprehend the determinants of biodiversity (Waide *et al.* 1999). Many ecological studies have shown that biomass is a surrogate for productivity (Mittelbach

et al. 2001, Bischoff *et al.* 2005), especially in herb-dominated communities like grasslands (Scurlock *et al.* 2002). Attempts to correlate species richness with the normalized difference vegetation index (NDVI, Gould 2000, Oindo and Skidmore 2002, Oindo *et al.* 2003) and pure hyperspectral reflectance (Carter *et al.* 2005) have been reported in the literature but, to our knowledge, no study exists that examines the relationship between species richness and biomass estimates derived from hyperspectral remote sensing data.

The main objective of our study was to develop a method, using field spectrometer data, for estimating aboveground biomass in grassland habitats along a dry-mesic gradient. The method should be independent of specific habitats or phenological period. A further aim was to investigate to what degree the calibrated biomass estimation could be scaled to hyperspectral data recorded from the Hyperion sensor, to evaluate the potential to scale models calibrated from plot-based estimates to larger landscapes as seen from space-borne sensors. Finally, a secondary objective was to use the estimated biomass distribution maps produced from the Hyperion scene to explore the relationship between species richness and biomass that is a central theme in ecological diversity studies.

2. Materials and methods

2.1 *Study area*

The study was conducted on the central part of the Swiss Plateau (8° 02′ E, 47° 25′ N) near the city of Aarau with an elevation ranging from 350 to 500 m. Grassland samples were collected from four characteristic, low-elevation grassland types (see table 1), previously mapped in a national mapping campaign (Eggenberg *et al.* 2001). The four semi-natural grassland types sampled (AE, AEMB, MBAE, MB) were purposely selected because of their differences in species composition and nutrient availability. These differences enabled the collection of a wider range of biomass samples. In particular, AE is a species-rich *Arrhenatherion*-type managed grassland, that is mesic and nutrient-rich. The mesic and species-rich type AEMB includes tall, dense and multilayered stands, composed of many grasses and several herb species, and is still comparably nutrient-rich (Eggenberg *et al.* 2001). The type MBAE stands between AEMB and MB in respect of species richness, nutrients and canopy height. Finally, true semi-dry MB grasslands (*Mesobromion* type) are comparably nutrient-poor and are generally dominated by *Bromus erectus* or *Brachypodium pinnatum* with stems standing well above the surrounding shorter herb vegetation. These stands are generally colourful and rich in herbs. The main management practice on the grasslands in the study area is production of hay, and very few areas are used as pastures.

Table 1. Description of the four grassland types sampled.

Type code	Phytosociology	Description
AE	Species-rich *Arrhenatherion* type	Mesic, species-rich, nutrient-rich, managed
AEMB	Transition *Arrhenatherion* to *Mesobromion*	Moderately mesic, species-rich
MBAE	Transition *Mesobromion* to *Arrhenatherion*	Moderately dry, species-rich
MB	*Mesobromion* type	Species-rich, semi-dry grassland

2.2 *Biomass–species richness sampling*

A total of 11 fields belonging to the four grassland types were selected from the existing national campaign map. The fields were chosen to have a total area larger than five Hyperion pixels and were checked for purity: only grasslands where the major vegetation type covered at least 75% of the mapped polygon were kept. Sampling was performed four times during the growing season of 2005 (10 June, 23 June, 28 July, 10 August). This was done to ensure that normally occurring variation due to phenology (Butterfield and Malmstrom 2009), canopy growth stage and management factors was recorded. Biomass samples were clipped at ground level using a 32 cm radius metal frame. Within each field, three randomly selected plots were sampled to account for the spatial variability of biomass. A total of 155 biomass samples were collected from the 11 grassland fields during the growing season of 2005. The collected material was stored in pre-weighed air-sealed plastic bags and brought to the laboratory where the total fresh biomass was measured. Samples were then dried in the oven at 65°C for 72 h and weighed again to measure the total dry biomass. The plant water content was calculated as the difference between fresh and dry weight. Finally, the mean value of the three fresh biomass samples collected at each field was assigned as the measured biomass at that field.

Grassland species richness data were extracted from a data set that was collected during a previous mapping project (Eggenberg *et al.* 2001) and covered scattered patterns throughout Switzerland. Aboveground biomass recorded in 2005 was related to plant species richness data recorded before 2001. It was not expected to see large differences in species richness patterns between pre-2001 and 2005. The grassland habitats under investigation have been given a protected status, thus management practices are regulated by law, and therefore no changes in land use (e.g. intensification of production) or in management practices that could have a subsequent (clear) effect on species composition and richness of these habitats are allowed. Furthermore, research on similar species-rich dry grasslands in Switzerland (Stampfli and Zeiter 2001, 2004), over periods of 10 and 13 years respectively, has shown that locally sampled species have persisted and were identified continuously during the whole period, and that no new species had invaded the study sites. Finally, with respect to the potential impact of extreme climatic conditions, in particular the summer drought of 2003, evidence from the 13-year study of Stampfli and Zeiter (2004) has shown that drought had an effect on the relative cover (i.e. abundance) of different species but not on the species composition, or on the number of species (species richness), which is investigated in this article. For every grassland field that was mapped in the national campaign, a circular sampling plot with a radius of 3 m was established and each individual plant species and its abundance were recorded. The total number of individual plant species at the sampling plot was recorded and used to express the species richness of the particular mapped grassland (Rocchini *et al.* 2007). A total of 106 grassland fields, with a maximum distance of 14 km from our sampling sites, were available within the Hyperion scene. These fields were selected and used for further analyses.

2.3 *Field spectral sampling for estimating aboveground biomass patterns in grassland habitats*

Parallel to biomass sampling, canopy spectral profiles of the grassland fields were collected using an Analytical Spectral Devices (ASD) FieldSpec Pro FR

spectroradiometer. This spectrometer has a 350–2500 nm spectral range and 1 nm spectral resolution, with a 25° field of view (ASD 2000). Collected spectra were converted to absolute reflectance by reference measurements over a Spectralon reflectance panel (Labsphere, North Sutton, NH, USA) with known spectral properties. Calibration of the spectrometer was made every 20 measurements to minimize changes in atmospheric condition. Measurements were collected under sunny and cloud-free conditions between 10:00 and 16:00, while walking along two diagonal transects across the length of each field. This resulted in 60–100 spectral measurements covering the whole extent of the grassland fields and not specifically the plots where biomass samples were collected. The ASD field spectra were then resampled to simulate Hyperion spectral bands using the spectral centre wavelength (CWL) and full-width half-maximum (FWHM) information for each individual Hyperion band (Barry 2001). After investigation for erroneous spectral measurements, the mean spectral reflectance of each grassland field was calculated as the mean of the 60–100 spectral measurements collected over the whole extent of the field.

2.4 *Hyperion imagery processing and analysis*

Hyperion radiometrically corrected (level 1R) data were acquired over the study area from a nadir (overhead) pass on 10 August 2005 at 10:06:49 Greenwich Mean Time (GMT). The EO-1 satellite has a sun-synchronous orbit at 705 km altitude. The Hyperion sensor collects 256 pixels with a spatial resolution of 30 m over a 7.65 km swath with a maximum acquisition length of 180 km. Data are acquired in 'pushbroom' mode with two spectrometers. One operates in the visible near infrared (VNIR) range (70 bands between 356 and 1058 nm with an average FWHM of 10.90 nm) and the other in the shortwave infrared (SWIR) range (172 bands between 852 and 2577 nm, with an average FWHM of 10.14 nm) (Pearlman *et al.* 2003). Of the 242 level 1R bands, 44 are set to zero by software (bands 1–7, 58–76, 225–242). The length of the Hyperion stripe for this particular study was 75 km.

After removal of Hyperion bands that (1) were set to zero, (2) were in the spectral range of 1350–1415 nm or 1800–1950 nm and thus seriously affected by atmospheric water vapour absorption or (3) overlapped between the two spectrometers, a total of 167 bands were available for further analysis (426–2355 nm). Post-processing of Hyperion level 1R data comprised correction for striping pixels, smoothing using a minimum noise fraction (MNF) transformation, atmospheric correction and image orthorectification. Correction for striping pixels and smoothing using forward and inverse MNF was applied as described by Datt *et al.* (2003). Atmospheric correction of the Hyperion data was performed using ATCOR-4 software (Richter 2003). Since the grassland fields were relatively flat and the field of view of the Hyperion sensor is small, topographic illumination effects were not accounted for. The following atmospheric parameters were selected for the correction: rural aerosol model, water vapour column of 1.0 g m^{-2} and visibility of 40 km. The resulting atmospheric correction yielded absolute reflectance differences for grassland surfaces between the Hyperion and the ASD measurements of 7% at 740 nm and 5% at 1500 nm. A digital terrain model (DTM) of Switzerland with a resolution of 25 m (Swisstopo 2007) was used for the orthorectification of the Hyperion scene. Analysis was performed with the software package PCI Geomatica Orthoengine, which uses the parametric sensor model (PCI Geomatics 2006). The nearest neighbour resampling method was used to preserve the original radiometry of the image (Eckert and Kneubühler 2004). Hyperion orbit and

scene parameters were selected and a total of 25 ground control points (GCPs) were collected, with an overall geo-registration error of 10.38 m.

2.5 *Statistical approaches for estimating aboveground grassland biomass*

The mean spectral reflectance of the 60–100 spectral measurements (collected with the ASD and then resampled to simulate Hyperion bands) and the mean biomass of the three samples collected at each grassland field were used in the statistical analysis. Biomass samples and spectral reflectance recorded at 11 grassland fields, repeated for four time steps during the 2005 growing season, were used to calibrate the statistical models. This was done to ensure that normally occurring variation in biomass and spectral reflectance due to vegetative growth stage or management practices on the different grassland types was included in the models. As a result, models could account for a larger temporal and across-grassland type variability than those calibrated using samples collected from only one date. Initial data screening revealed a heavily skewed distribution of the biomass data. Therefore, to improve the regression modelling, the biomass data were log-transformed to approach a normal distribution.

The relationship between biomass and several hyperspectral and broadband VIs was investigated. These were VIs (see table 2 for abbreviation) related to vegetation structure (NDVI, RDVI, SR, SAVI, TSAVI, OSAVI and MTVI1), to vegetation water status (NDWI, SRWI, PWI and WDVI), to chlorophyll and the red edge (RESP, GMI, CI_1, CI_2, VOGa, VOGb, VOGc, MCARI and TRVI) and other features (CAI, CAI_ATSAVI, TVI and PRI), which themselves are related to biomass. A detailed description of the properties and advantages of these VIs can be found in Broge and Leblanc (2001), Haboudane *et al.* (2004) and Zarco-Tejada *et al.* (2005). All VIs were used individually but also in combination with each other, to calibrate linear and multiple linear regression models to explain the biomass sampled in the field. Multiple linear regressions models were calibrated using VIs that were only weakly correlated ($r \leq 0.5$) to avoid collinearity problems.

Most of the above-mentioned VIs consider only certain parts of the spectrum, primarily the chlorophyll absorption region (680 nm), the near-infrared (NIR) reflectance (800 nm) and/or the green reflectance peak (550 nm). Given this limitation, and in an attempt to use the depth of information included in the large number of bands of hyperspectral data, we built narrowband NDVI-type indices ($\text{nb\_NDVI}_{\text{type}}$) (Thenkabail *et al.* 2000) as shown in equation (1):

$$\text{nb\_NDVI}_{\text{type}}[b_1, b_2] = \frac{b_1 - b_2}{b_1 + b_2}. \tag{1}$$

All possible two-pair combinations were used in equation (1), where b_1 and b_2 were the Hyperion simulated bands from the field reflectance measurements. A total of 27 889 narrowband indices were calculated. These indices were used in linear regression models to determine their predictive power to explain measured biomass.

The disadvantage of existing VIs and of the $\text{nb\_NDVI}_{\text{type}}$ indices is that they only consider very few of the available hyperspectral bands. Although much of the information provided by neighbouring bands is often redundant (Thenkabail *et al.* 2004), it is still possible that the spectral information is not optimally used by these indices. Therefore, multiple linear regression (MLR) that selected the best combination of linear predictors from the Hyperion simulated bands was used for biomass

Table 2. Vegetation indices for estimating aboveground biomass investigated in this study.

Vegetation index	Equation	Reference
	Structural Indices	
Normalized difference vegetation index (NDVI)	$NDVI = (R_{NIR} - R_{red})/(R_{NIR} + R_{red})$	(Rouse *et al*. 1974)
Renormalized difference vegetation index (RDVI)	$RDVI = (R_{800} - R_{670})/\sqrt{(R_{800} + R_{670})}$	(Rougean and Breon 1995)
Simple ratio index (SR)	$SR = R_{NIR}/R_{red}$	(Rouse *et al.* 1974)
Soil-adjusted vegetation index (SAVI)	$SAVI = (1 + L)(R_{800} - R_{670})/(R_{800} + R_{670} + L)$ $(L = 0.5)$	(Huete 1988)
Transformed soil-adjusted vegetation index (TSAVI)	$TSAVI = \alpha\,(R_{NIR} - \alpha R_{red} - b)/$ $(\alpha R_{NIR} + R_{red} - \alpha b + X(1 + \alpha^2))$, where α = slope of the soil line, b = soil line intercept and X = adjustment factor to minimize soil noise.	(Baret and Guyot 1991)
Optimized soil-adjusted vegetation index (OSAVI)	$OSAVI = (1 + 0.16)\,(R_{800} - R_{670})/$ $(R_{800} + R_{670} + 0.16)$	(Rondeaux *et al*. 1996)
Modified triangular vegetation index (MTVI1)	$MTVI1 = 1.2\,[1.2\,(R_{800} - R_{550}) - 2.5\,(R_{670} - R_{550})]$	(Haboudane *et al*. 2004)
	Water indices	
Normalized difference water index (NDWI)	$NDWI = (R_{860} - R_{1240})/(R_{860} + R_{1240})$	(Gao 1996)
Simple ratio water index (SRWI)	$SRWI = R_{850}/R_{1240}$	(Zarco-Tejada *et al.* 2003)
Plant water index (PWI)	$PWI = R_{970}/R_{900}$	(Peñuelas *et al*. 1997)
Weighted difference vegetation index (WDVI)	$WDVI = R_{red} - \alpha R_{NIR}$, where α = slope of the soil line	(Clevers 1991)
	Chlorophyll and red-edge indices	
Red-edge spectral parameter (RESP)	$RESP = R_{750}/R_{710}$	(Vogelmann *et al*. 1993)
Gitelson and Merzlyak index (GMI)	$GMI = R_{750}/R_{550}$, $GM2 = R_{750}/R_{700}$	(Gitelson *et al*. 2003)
Carter indices	$CI\_1 = R_{695}/R_{420}$, $CI\_2 = R_{695}/R_{760}$	(Carter 1994)
Vogelmann indices	$VOGa = (R_{740})/(R_{720})$ $VOGb = (R_{734} - R_{747})/(R_{715} + R_{726})$ $VOGc = (R_{734} - R_{747})/(R_{715} + R_{720})$	(Vogelmann *et al.* 1993)

(*Continued*)

Table 2. (*Continued*).

Vegetation index	Equation	Reference
Modified chlorophyll absorption ratio index (MCARI)	$MCARI = ((R_{700} - R_{670}) - 0.2\,(R_{700} - R_{550}))\,(R_{700}/R_{670})$	(Daughtry *et al.* 2000)
Triangular vegetation index (TRVI)	$TVI = 0.5\,[120(R_{750} - R_{550}) - 200(R_{670} - R_{550})]$	(Broge and Leblanc 2001)
Photochemical reflectance index (PRI)	$PRI = (R_{528} - R_{567})/(R_{528} + R_{567})$	(Gamon *et al.* 1992)
	Other indices	
Cellulose absorption index (CAI)	$CAI = 0.5\,(R_{2000} + R_{2200}) - R_{2100}$	(Nagler *et al.* 2003)
Litter-corrected adjusted transformed soil-adjusted vegetation index (CAI_ATSAVI)	$CAI\_ATSAVI = \frac{a(R_{800} - aR_{670} - b)}{aR_{800} + R_{670} - ab + X(1+a^2) + L \times CAI}$ where α = slope of the soil line, b = soil line intercept, X = adjustment factor to minimize soil noise.	(He *et al.* 2006)
Transformed vegetation index (TVI)	$TVI = \sqrt{(R_{NIR} - R_{RED})/(R_{NIR} + R_{RED})^{+0.5}}$	(Deering *et al.* 1975)

Notes: Detailed description of the properties and advantages and references of these VIs can be found in Broge and Leblanc (2001), Haboudane *et al.* (2004) and Zarco-Tejada *et al.* (2005). R_x corresponds to the reflectance recorded at wavelength x.

estimation. Branch-and-bound (Miller 2002) variable search algorithms were chosen to identify spectral bands that best explained biomass variability. A branch-and-bound algorithm searches the complete space of solutions for a given problem for the best solution. Since explicit enumeration is normally impossible owing to the exponentially increasing number of potential solutions, the use of bounds for the function to be optimized combined with division of sets of solutions into subsets enables the algorithm to search parts of the solution space only implicitly (Clausen 1999). In this study, models were built using one to four spectral bands, in an attempt to avoid multicollinearity (Curran 1989, De Jong *et al.* 2003) or overfitting of the models (Crawley 2005), and because preliminary results showed that accuracies improved only marginally when using more than four bands.

The overall capability of each model to explain the variability in the biomass samples was evaluated by the adjusted coefficient of determination (adj.R^2) (Hill and Lewicki 2006). Adj.R^2 was used since it will only increase if the new variable added will improve the model more than would be expected by chance (Crawley 2005). The model prediction error for estimating biomass was assessed by using a four-fold cross-validation (CV) (Diaconis and Efron 1983). The four-fold cross-validation randomly split all mean biomass measurements per grassland field ($n = 50$) into four bins, then it iteratively determined regression parameters using a sample of three bins and tested the resulting model on the remaining bin. This procedure was repeated until each bin had been left out once. Since predicted samples were not used to build the model, the calculated cross-validation root mean square error (CV-RMSE) is a good indicator of the model accuracy and predictive power. In addition, to investigate the effect of seasonal variability on the predictive power of the models, a four-fold 'date' CV procedure was used. For this, models were calibrated using data collected from three dates and then their predictions validated with data collected on the fourth. This process was repeated four times until each date had been used once for validation of model predictions.

2.6 *Up-scaling of field-calibrated models*

Statistical models with the highest accuracy and predictive power were up-scaled to the geometrically and atmospherically corrected Hyperion scene to predict the spatial distribution of biomass over the study area. Owing to the differences between the two instruments (ASD–Hyperion), certain measures had to be taken to ensure accurate spectral and spatial scaling of these models. Spectral up-scaling was achieved by resampling the ASD spectral bands to simulate those of the Hyperion sensor before any regression modelling was performed, and by applying atmospheric correction to the acquired Hyperion scene. Thus, the at-sensor radiance recorded by the Hyperion sensor was transformed to top-of-canopy reflectance after accounting for solar and sensor geometries, atmospheric optical properties and sensor band specifications (Richter 2003). To account for the 30 m spatial resolution of the spectral signal recorded by the Hyperion sensor, each grassland was assigned the aggregated mean signal of the 60–100 spectral signatures collected with the ASD spectroradiometer along transects over the whole extent of the field. In addition, to ensure the 'purity' of the Hyperion pixels extracted from the scene, a procedure was followed to only select pixels from the centre of the grassland field. In particular, a buffer of 17 m towards the centre of the grassland field was created, and any pixel whose centre was within this area was removed from further analyses. Thus, pixels adjacent to the edges of the fields

were excluded since chances were high that the spectral signal recorded was mixed with the contribution of other land-use types. Finally, to deal with the spatial scaling difference between the 30 m Hyperion pixel size and the relatively small size of the biomass sampling plots, we averaged the multiple biomass samples within each of the grasslands and assigned this value to the whole grassland field (White *et al.* 1997). This was done because sampling of biomass was performed within already mapped and outlined grassland fields (Eggenberg *et al.* 2001). The borders of these fields were primarily identified via aerial photograph interpretation, and then every field was visited by field teams, who updated, if required, the pre-selected borders so that the grassland area was homogeneous from structural and species composition perspectives across the whole extent of its area. It was within this extent of these grassland polygons that biomass samples were taken.

On the date of the Hyperion data acquisition, two sources of canopy reflectance measurements existed for the sampled grassland fields, that is, reflectance measurements from the ASD field spectroradiometer (that were resampled to simulate Hyperion spectral bands) and reflectance measurements from the Hyperion sensor. Therefore, VIs and nb_NDVI$_{type}$ indices were calculated for the sampled grasslands using both the ASD and the Hyperion sensor reflectance measurements. Then, differences (measured in RMSE) between the absolute reflectance, VIs and the nb_NDVI$_{type}$ indices derived from these two sources were calculated. Only models whose predictors (VIs, nb_NDVI$_{type}$ indices, absolute reflectance) had the smallest differences between the ASD and the Hyperion sensor estimates were selected. These models were subsequently used to up-scale biomass predictions to the Hyperion scene and to create the biomass distribution maps across the landscape. Finally, biomass estimates for 106 grassland fields, where species richness data were available, were extracted.

While we recognize that empirical regressions between biophysical parameters and reflectance or VIs are limited to the place and time over which the ground data are collected (Verstraete *et al.* 1996) we believed that this did not pose a problem with upscaling the biomass prediction models following the above-mentioned methodology. This is because extracted biomass estimations were restricted only to comparable low-elevation grassland types growing under the same environmental and management conditions as the grasslands from where our samples were collected.

3. Results

A summary of the biomass measurements is reported in table 3 and figure 1. The highest variability of biomass was observed at the first (10 June) and second (23 June) sampling dates. Sampled grasslands represent a dry-mesic gradient having different availabilities of water and nutrients, which eventually lead to different rates of growth and biomass accumulation. Lower biomass variability observed later in the season could be partly attributed to the management practices applied to these fields. Furthermore, analyses on the individual biomass samples collected showed that the average standard deviation of the three samples was 21% of the mean biomass measured within each grassland field.

The best five models from the different VI categories for predicting biomass are presented in table 4. Overall, models developed with existing VIs gave low adj.R^2 values. Higher values were obtained by VIs related to canopy water content (e.g. NDWI, adj.$R^2 = 0.33$).

Table 3. Summary statistics for original and log-transformed measured biomass at 50 grassland fields over four time steps during the 2005 growing season.

	Biomass					
	n	Mean	Std	Min	Max	Range
Original measurements (kg m^{-2})	50	0.7756	0.5704	0.1785	3.3180	3.1395
Log-transformed measurements log(kg m^{-2})	50	−0.4523	0.6186	−1.7230	1.1990	2.9220

Note: Std, standard deviation.

Models using VIs that minimize the soil background influences in the spectral signal, like TSAVI (Baret *et al.* 1989), did not improve the results (adj.$R^2 = 0.28$), while models using the traditional NDVI and a modified version of it that is more suitable for low and high LAI values (RDVI) (Haboudane *et al.* 2004) gave similar adj.R^2 (0.29, 0.28 for NDVI and RDVI respectively). Comparably poor results (adj.$R^2 = 0.28$) were also obtained using the Carter index 2 (CI_2), which had been found to indicate plant stress (Carter 1994). Calibration of linear regression models using more than one VI did not improve biomass predictions, thus no results thereof are presented below.

All possible two-band combinations were used to create nb_$NDVI_{type}$ indices. Results for the adj.R^2 achieved between biomass and each nb_$NDVI_{type}$ index are graphically presented in figure 2. Values for adj.R^2 ranged from 0.01 to 0.74, reflecting a wide variation in the strength of the relationship between nb_$NDVI_{type}$ indices and biomass. Highest adj.R^2 values were observed for nb_$NDVI_{type}$ indices with wavelengths from the NIR and the SWIR namely: 720, 1200, 1700 and 2280 nm. The best $NDVI_{type}$ index model for each one of the above four regions is presented in table 4.

Results of the best two MLR models for each number of predictors (one to four bands) that were identified from the exhaustive branch-and-bound selection algorithm are reported in table 4. Adj.R^2 ranged from 0.52 for one-band models to 0.86 for four-band models. Primarily, the bands selected by these analyses were in the spectral regions of 478, 518, 1205 and 2235 nm.

The overall performance of the above models to predict biomass was also evaluated. Cross-validated biomass prediction errors (CV-RMSE) of the best VIs, nb_$NDVI_{type}$ indices and MLR models are presented in figure 3 and table 4. Models that used existing VIs predicted comparably poorly, with CV-RMSE from ~ 0.55 to ~ 0.52 log(kg m^{-2}) of biomass. The new nb_$NDVI_{type}$ indices improved the predictive power of the models by reducing the CV-RMSE to 0.36 log(kg m^{-2}). These predictions were superior to one-band MLR models that had a CV-RMSE of 0.42 log(kg m^{-2}). Inclusion of additional bands in the MLR models further increased their predictive power by reducing the CV-RMSE to 0.31, 0.27 and 0.24 log(kg m^{-2}) for two, three and four band MLR models, respectively.

Overall, models calibrated with biomass samples collected on the first two sampling dates of the season (date 1 = 10 June, date 2 = 23 June) predicted biomass with lower RMSE contrary to models calibrated using samples from only one of these dates that gave poorer predictions. For example, the best nb_$NDVI_{type}$ index model for estimating biomass when calibrated with samples from dates 1 and 2

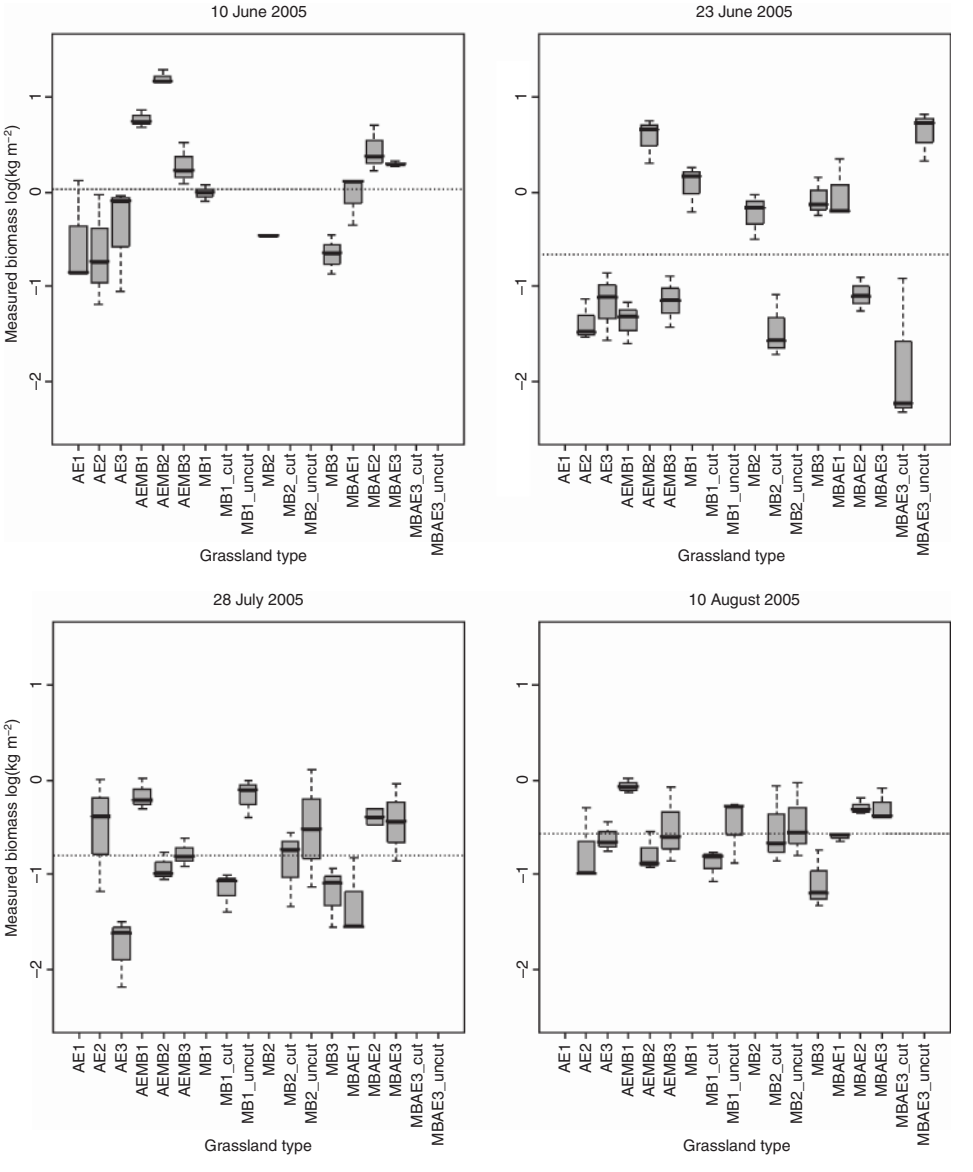

Figure 1. Mean biomass (log(kg m^{-2})) measurements of individual sampled fields during the growing season. Dashed horizontal lines represent the mean biomass measured per sampling date.

(C-1,2,4/V-3, C-1,2,3/V-4) yielded RMSE of 0.30 and 0.34 log(kg m^{-2}). On the contrary, when the model was calibrated with samples from late dates in the season (C-2,3,4/V-1, C-1,3,4/V-2; date 3 = 28 July, date 4 = 10 August), it was not able to extrapolate to the large range of biomass observed early in the season and thus created higher 'date' cross-validated errors. In particular, RMSE of biomass prediction increased to 0.46 and 0.43 log(kg m^{-2}).

For the date of the Hyperion data acquisition, differences between model predictors (VIs, nb_NDVI_{type} indices, absolute reflectance) calculated using ASD field

Table 4. Adjusted coefficient of determination (adj.R^2) and cross-validated biomass prediction error (CV-RMSE) of the best models calibrated with biomass (log(kg m^{-2})) and spectral information (VIs, nb_$NDVI_{type}$ indices, MLR), collected at 50 grassland fields over the whole growing season using an ASD field spectroradiometer, with bands resampled to simulate those of the Hyperion band widths.

Model	Adj.R^2 of models calibrated from ASD field spectral measurements	CV-RMSE of predicted biomass from ASD field spectral measurements
NDWI	0.33	0.51
TSAVI	0.29	0.53
RDVI	0.29	0.52
NDVI	0.28	0.53
CI_2	0.28	0.52
nb_$NDVI_{type}$ b1326, b1710	0.65	0.36
nb_$NDVI_{type}$ b1084, b1205	0.56	0.39
nb_$NDVI_{type}$ b1074, b2264	0.52	0.41
nb_$NDVI_{type}$ b722, b1669	0.51	0.42
MLR-1 band b1710	0.52	0.42
MLR-1 band b1699	0.51	0.43
MLR-2 band b478, b1780	0.77	0.31
MLR-2 band b468, b1780	0.77	0.31
MLR-3 band b518, b1699, b1710	0.82	0.27
MLR-3 band b1185, b1205, b1235	0.82	0.29
MLR-4 band b518, b1205, b1235, b1710	0.86	0.22
MLR-4 band b518, b1215, b1225, b1720	0.86	0.24

spectral measurements and spectral measurements from the Hyperion sensor, for nine sampled grassland fields, are reported in table 6. The smallest difference between field–sensor calculated model predictors was observed for the b1084 nm-b1205 nm nb_$NDVI_{type}$ index. Overall, differences were lower between field–sensor calculated VIs and nb_$NDVI_{type}$ indices than between field–sensor measured reflectance.

Using the spectral recordings of the Hyperion sensor and the statistical models developed with seasonal spectral and biomass field measurements, biomass of nine grassland fields was predicted on the date of the Hyperion data acquisition. Results of the RMSE between predicted and actual biomass measured on these nine grassland fields are presented in table 7. The smallest prediction RMSE was observed for the b1084 nm-b1205 nm nb_$NDVI_{type}$ index model, with 0.25 log(kg m^{-2}) of biomass.

This model was chosen for up-scaling biomass estimations to the Hyperion scene because of its small prediction error, but also since Datt *et al.* (2003) reported that VIs calculated using Hyperion bands from the NIR region had minimal absolute value differences from those calculated from ASD reflectance measurements on the ground. Even though using a ratio composed only of NIR bands could cause a conflict with the high NIR reflectance of soils in arid or semi-arid areas, Geerken *et al.* (2005) stated that this would not be a problem in areas that have already been identified as being covered by vegetation, like our grassland fields. The resulting map of the biomass distribution of the grassland habitats within our study area is presented in figure 4, and shows distinct differences in biomass patterns across the landscape. Using this map of biomass distribution, estimates for the 106 mapped grasslands were extracted.

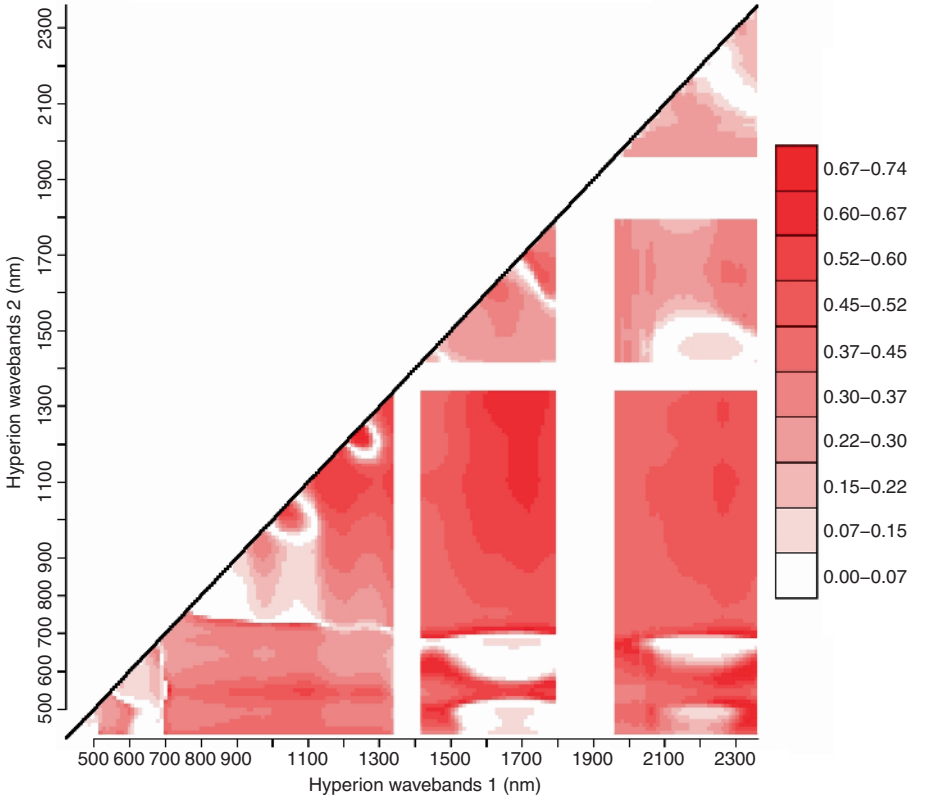

Figure 2. Result of the narrowband NDVI-type vegetation index analyses (nb_NDVI_{type}). The graph shows the adjusted coefficient of determination (adj.R^2) from the regression of biomass against the nb_NDVI_{type} indices, calculated from any band pairs among the simulated Hyperion bands. Light red areas indicate higher adj.R^2. White gaps represent water absorption regions that were removed from the analysis.

The relationship between biomass estimates and the species richness recorded for these grasslands is presented in figure 5.

4. Discussion

The main purpose of this study was to explore the potential of hyperspectral remote sensing for mapping aboveground biomass in grassland habitats along a dry-mesic gradient, independent of a specific type or phenological period. Several statistical models were developed to serve this objective.

Even though models using existing VIs gave low adj.R^2 values, our results indicated that higher values were obtained by VIs related to canopy water content. This can be explained by the strong relationship between canopy water content and biomass (Mutanga *et al.* 2003, Anderson *et al.* 2004). Asner (1998) has shown that an increase in biomass leads to an increase in canopy water content. Furthermore, the reason why VIs that minimize the soil background influences did not improve the models can mainly be attributed to the fact that the grasslands sampled for this study are rich in

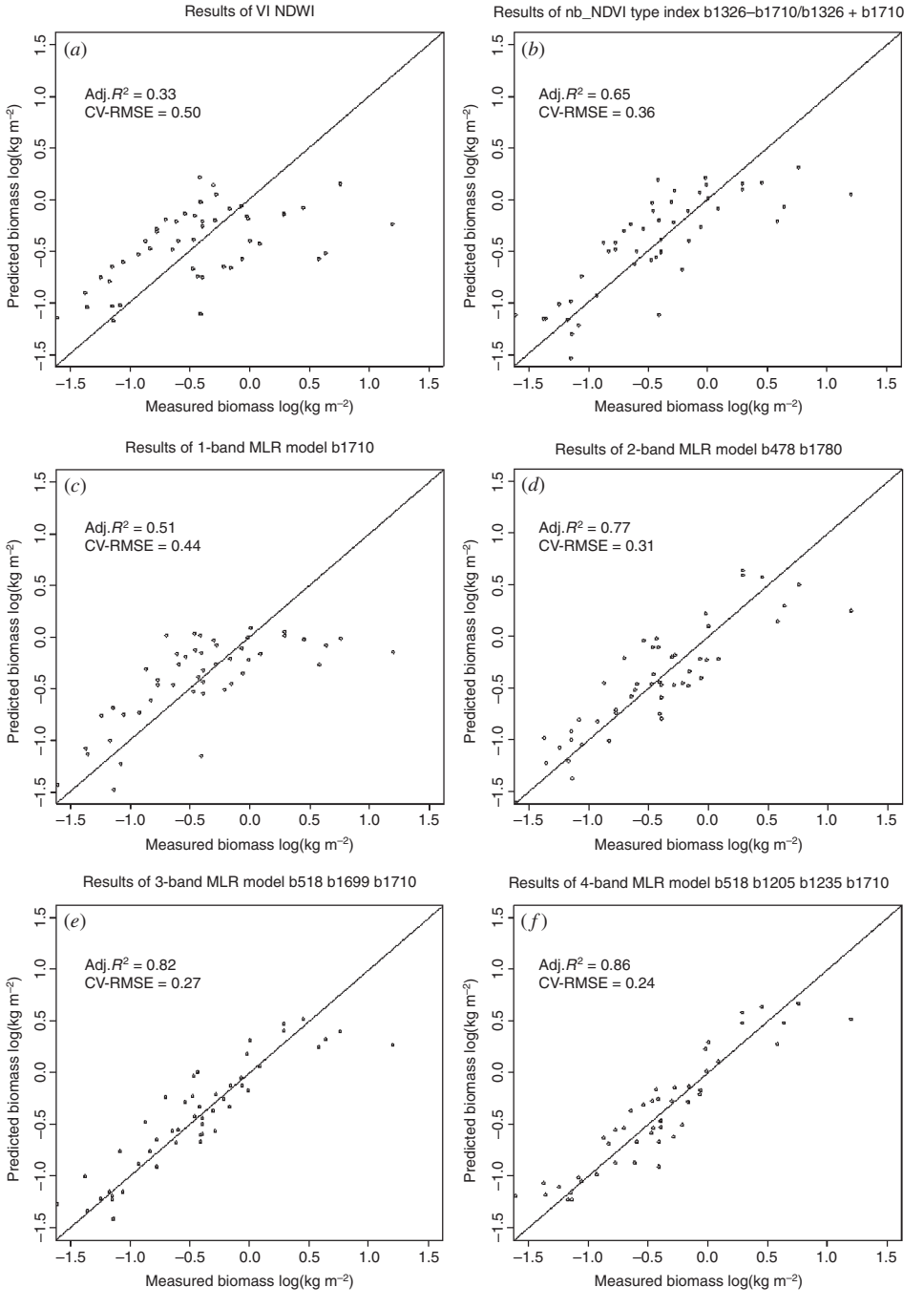

Figure 3. Best measured vs predicted biomass estimates from regression models of (*a*) existing VIs, (*b*) nb_NDVI$_{type}$, and (*c*)–(*f*) one to four spectral band MLR, optimized with a four-fold cross-validation using samples from all four sampling dates. Biomass values are in logarithmic scale.

Table 5. Biomass (log(kg m^{-2})) prediction errors of best models built with three approaches. Models were calibrated on three dates and validated on the fourth. C-2,3,4/V-1 means that regression models were calibrated on dates 2, 3 and 4 and validated on date 1. Recording dates were date 1 = 10 June; date 2 = 23 June; date 3 = 28 July and date 4 = 10 August.

	RMSE					
	Existing VIs	nb_NDVI_{type}	1-band MLR	2-band MLR	3-band MLR	4-band MLR
Calibration-validation dates	NDWI	nb_NDVI_{type} b1326, b1710	MLR-b1710	MLR-b478, b1780	MLR-b1185, b1205, b1235	MLR- b518, b1205, b1235, b1710
C-2,3,4/V-1	0.61	0.46	0.57	0.4	0.35	0.31
C-1,3,4/V-2	0.62	0.43	0.49	0.35	0.28	0.38
C-1,2,4/V-3	0.47	**0.30**	**0.36**	**0.21**	**0.18**	**0.15**
C-1,2,3/V-4	**0.45**	0.34	0.45	0.27	0.25	0.24
Resubstitution-RMSE	0.49	0.39	0.42	0.28	0.25	0.21

Note: Bold numbers correspond to the lowest prediction error for each model.

Table 6. RMSE between spectral reflectance, VIs and nb_NDVI_{type} indices calculated using spectral measurements collected in the field with an ASD and spectral measurements from the Hyperion sensor, for nine grassland fields sampled at the date of the Hyperion data acquisition. RMSE between field and sensor-estimated VIs and nb_NDVI_{type} indices are expressed as the percentage (%) of their possible value range. Possible value range for VIs and nb_NDVI_{type} indices is 0–1 and for spectral reflectance 0–100. Since CI_2 is a ratio index and not a normalized difference index, the RMSE between field and sensor estimates is expressed as a percentage of the observed value range of CI_2 calculated using ASD field spectral measurements.

Model predictors	RMSE between field-measured and Hyperion-derived model predictors (reflectance and indices) %
NDWI	5
TSAVI	10
RDVI	9
NDVI	8
CI_2	11
nb_NDVI_{type} b1326, b1710	7
nb_NDVI_{type} b1084, b1205	3
nb_NDVI_{type} b1074, b2264	8
nb_NDVI_{type} b722, b1669	8
MLR-1 band b1710	4.9
MLR-1 band b1699	5
MLR-2 band b478, b1780	1.4/4.1
MLR-2 band b468, b1780	2.1/4.1
MLR-3 band b518, b1699, b1710	1.1/5/4.9
MLR-3 band b1185, b1205, b1235	9.6/11.8/11.5
MLR-4 band b518, b1205, b1235, b1710	1.1/11.8/11.8/4.9
MLR-4 band b518, b1215, b1225, b1720	1.1/11.6/11.3/5.3

Table 7. Biomass (log(kg m^{-2})) prediction errors (RMSE) for nine grassland fields at the date of the Hyperion data acquisition (10 August 2005). Hyperion sensor spectral measurements were used to predict biomass according to the field-calibrated regression models.

Model	RMSE of biomass predicted from Hyperion sensor spectral measurements
NDWI	0.28
TSAVI	0.33
RDVI	0.41
NDVI	0.32
CI_2	0.29
nb_NDVI_{type} b1326, b1710	0.70
nb_NDVI_{type} b1084, b1205	0.25
nb_NDVI_{type} b1074, b2264	0.35
nb_NDVI_{type} b722, b1669	0.40
MLR-1 band b1710	0.43
MLR-1 band b1699	0.44
MLR-2 band b478, b1780	2.72
MLR-2 band b468, b1780	3.92
MLR-3 band b518, b1699, b1710	1.71
MLR-3 band b1185, b1205, b1235	3.10
MLR-4 band b518, b1205, b1235, b1710	1.94
MLR-4 band b518, b1215, b1225, b1720	2.79

herbs and have high canopy cover during the growing season (Eggenberg *et al.* 2001), thus soil reflectance was minimal.

An important finding of this study was that our analyses using nb_NDVI_{type} indices identified regions from the NIR and the shortwave infrared (SWIR) that resulted in more accurate models for estimating biomass than do existing VIs that primarily use the red and NIR regions. Specifically, the best nb_NDVI_{type} indices used the wavelengths 720, 1200, 1700 and 2280 nm. The 720 nm is the red-edge part of the spectrum, where the maximum change in the slope of the vegetation reflectance spectra occurs (Filella and Peñuelas 1994, Thenkabail *et al.* 2000). Vegetation stress is best detected in the red-edge region (Elvidge and Chen 1995, Thenkabail *et al.* 2004) and additional information about chlorophyll and nitrogen status of plants can be extracted (Carter 1994, Elvidge and Chen 1995, Clevers and Jongschaap 2001). The other regions (1200, 1700 and 2280 nm) are strongly associated with plant leaf water content, which is correlated with canopy biomass and LAI (Hunt 1991) and to cellulose, starch, lignin and nitrogen concentrations (Kumar *et al.* 2001). In particular, Asner (1998) has shown that the water absorption feature around 1200 nm (Curran 1989) exhibits an obvious deepening as LAI and subsequently biomass are increasing. Our results confirm findings of earlier studies (Cook *et al.* 1989, Hunt 1991, Gong *et al.* 2003) that correlate the ratio between NIR and SWIR to productivity and LAI. Additionally, Geerken *et al.* (2005) have shown that strongest correlations between biomass of annual grasses and narrowband indices were found between NIR-NIR and NIR-SWIR constructed narrowband ratios.

Another finding of our study was that MLRs using the exhaustive branch-and-bound selection algorithm were successful in estimating aboveground biomass. Although the selection of spectral bands was solely based on statistical optimization, these bands were primarily located at key spectral regions with respect to physical

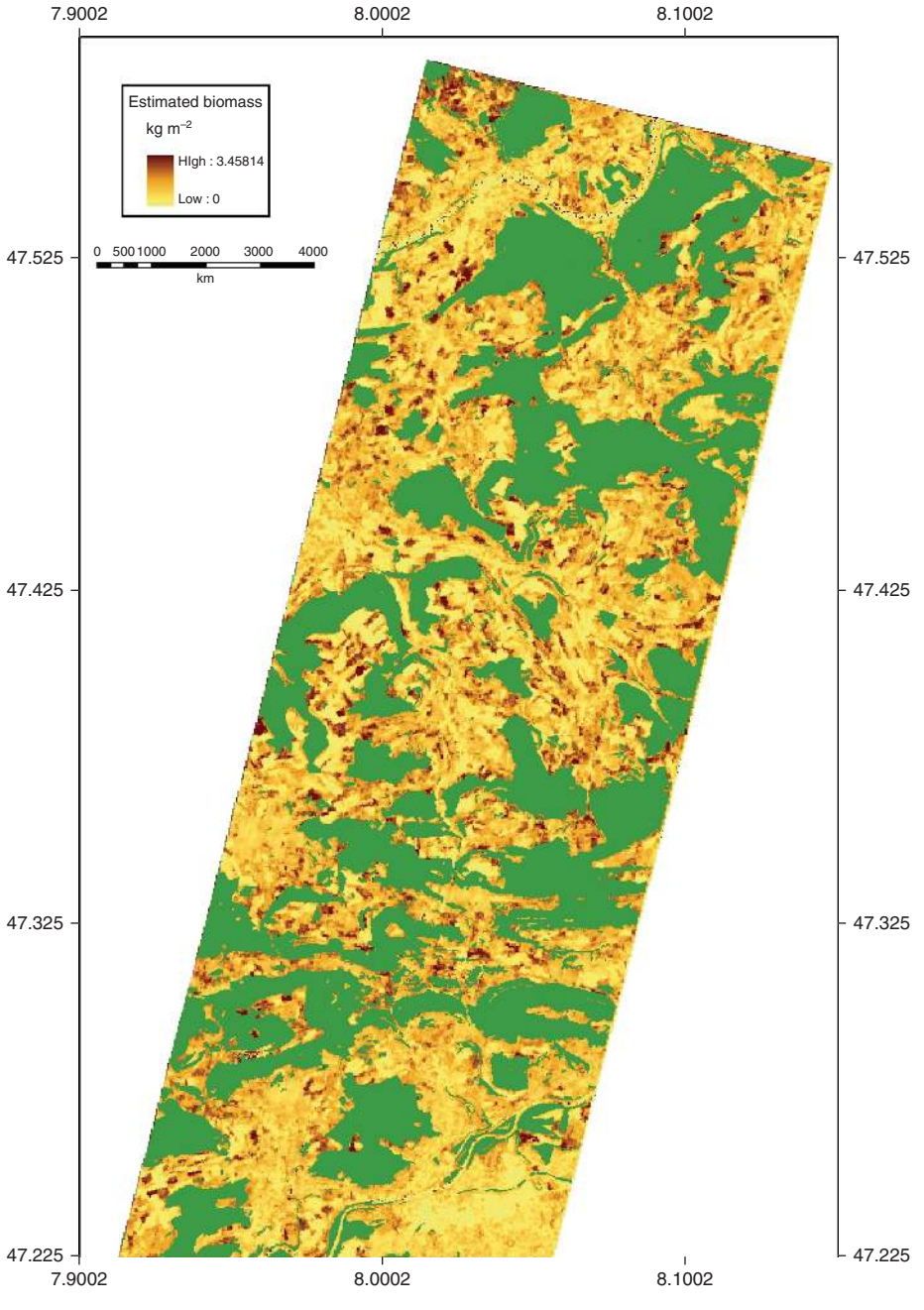

Figure 4. Biomass prediction map (kg m^{-2}) created using Hyperion spectral band values, using an nb_NDVI$_{type}$ index regression model constructed with bands at b1084 nm and b1205 nm. Forest areas are masked with green.

processes of plants and vegetation biomass. The 478 and 518 nm bands from the visible region are highly correlated with chlorophyll content of vegetation (Curran 1989, Kumar *et al.* 2001), the 1205 nm band from the NIR and the 1710 nm band

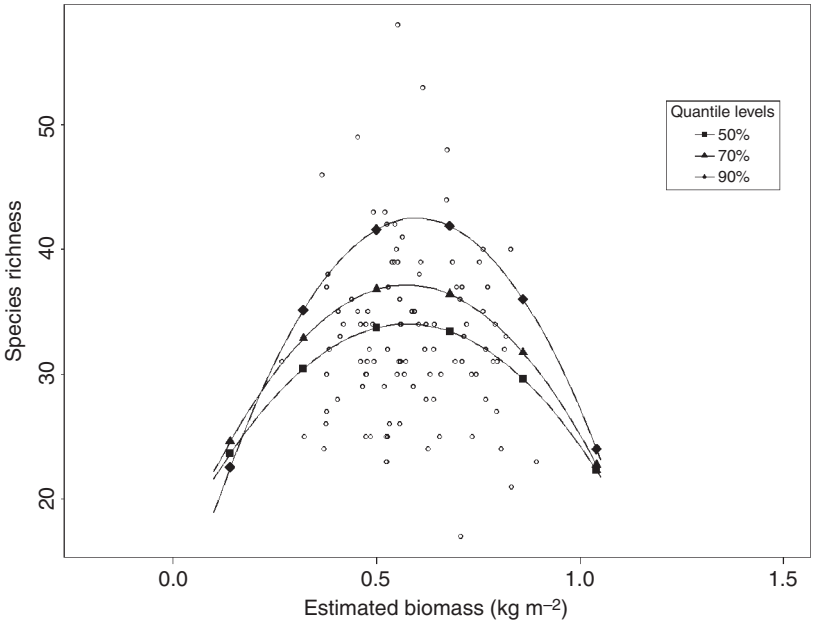

Figure 5. Relationship between species richness and biomass estimated from the b1084 -b1205 nm nb_NDVI$_{type}$ index model. The quantile regression models are of type: richness = b0 + b1biomass + b2biomass^2, between species richness and estimated biomass for 106 grassland fields. The mean (50% quantile) represents a simple quadratic regression model, while the higher quantiles represent a model fit through the top 30% (70% quantile) and the top 10% (90% quantile) of the data range.

from the SWIR are related to plant moisture and leaf mass (Hunt 1991, Asner 1998, Thenkabail *et al.* 2004). Finally, the 2235 nm band has been related to biochemical canopy properties like cellulose, starch and lignin concentrations (Elvidge 1990). Even though different MLR models used slightly different bands, these were neighbouring and highly correlated to the ones mentioned above, and thus provided the same type of information. In general, MLR can be considered a successful approach to optimize the retrieval of physical properties from spectral information.

The results of this study indicate the importance of using multiple dates for calibrating models in order to capture a large range of variability and to increase model stability. In particular, results from the four-fold 'date' CV analyses showed a clear pattern; models calibrated with biomass samples collected on the first two sampling dates of the season predicted biomass with higher accuracy. The reason for this pattern probably originated from the high variability of the biomass samples collected on date 1 and date 2 (figure 1). At the beginning of the season, vegetation is developing at different rates, which yields differences in biomass accumulation, percentage of canopy closure and, subsequently, differences in spectral reflectance (Jensen 2000). Spectral and biomass sampling on these dates captured differences between the grassland types along a dry-mesic gradient. Thus, models calibrated with data from these dates could account for a much broader range of variability of biomass with relation to spectral reflectance.

In addition, our analyses showed that it was possible to up-scale field-developed statistical models to the Hyperion sensor level for estimating biomass at the landscape scale. The smallest differences between field–sensor calculated model predictors

were observed for VIs and nb_NDVI$_{type}$ indices (see table 6). Vegetation indices can minimize external effects such as atmosphere, sun and viewing angle, and thus normalize effects like canopy background variation and soil variations (Jackson and Heuete 1991). Additionally, differences in absolute reflectance recorded in the field and recorded by the sensor were higher in the NIR and SWIR compared to the visible (VIS) region of the spectrum. We attribute this to a poor calibration of the SWIR spectrometer of the Hyperion sensor and to difficulties in the atmospheric correction of the data. Lack of knowledge on the exact state of the atmosphere at the date of the acquisition and, in particular, not accurate information on parameters like water vapour content, has been found to have a more pronounced effect on the near and shortwave infrared parts of the spectrum (Liang 2004). With respect to model predictive power, except for MLR models using two or more spectral bands, all other models produced comparable low biomass prediction RMSE. The main reason for these small RMSEs was that statistical models were calibrated with measurements of biomass and spectral reflectance which were collected and transformed in such a way that they matched the spectral and spatial resolution of the Hyperion sensor. In particular, biomass samples were randomly selected within the extent of a homogeneous area and then were averaged to represent a single value per field, while ASD wavebands were resampled to simulate Hyperion spectral bands. Furthermore, the sensor-predicted biomass per field was the aggregated estimation of all 'pure' pixels within the grassland field. The smoothing effect of this aggregation reduced the variance of estimated biomass. Thus the value approached that of the field measurement, being the mean of several biomass measurements on the grassland field.

Finally, results of this study showed the potential of hyperspectral remote sensing for exploring plant species richness patterns of grassland habitats. The relationship between predicted grassland biomass and species richness appeared to be unimodal, with species richness peaking at intermediate levels of biomass. Our results agree with a number of ecological studies that have related plant biomass as a measure of productivity with plant diversity (e.g. Mittelbach *et al.* 2001) and have identified a hump-shaped (unimodal) relationship. The explanation for that relationship is that at low levels of productivity or high disturbance, fewer species can survive, hence richness is lower. Alternatively, at high levels of productivity or low disturbance, comparably few species can monopolize the available resources and outcompete other species. It is only at intermediate levels of productivity or moderate disturbance that species richness is peaking (Palmer and Hussain 1997). Our results show that higher species richness is mainly observed at intermediate levels of biomass. However, this relationship is not statistically significant since there are a number of low species richness values at intermediate biomass levels as well. The main reason for this is possibly related to the time during the growing season when the Hyperion scene was acquired. In particular, many of the highly productive grasslands (and thus the ones with low species richness) were already cut and were at the stage of accumulating new biomass. Therefore, the estimated biomass from the Hyperion scene did not reliably represent the productivity of these grassland habitats. We believe that these grasslands would have been towards the highly productive end of the unimodal curve if the scene had been acquired earlier, and in particular at the peak of the growing season.

5. Conclusions

The results presented in this article demonstrate the potential of hyperspectral remote sensing for estimating biomass of grassland habitats throughout a whole growing

season. Our analyses actually highlight the importance of acquiring multitemporal spectral and biomass measurements especially at the beginning of the growing season, in order to capture a larger range of biomass and seasonal variability and therefore to be able to create reliable and phenology-independent models. An additional conclusion of this study is that appropriate spectral and spatial scaling of field observations can assist towards successful up-scaling of field-developed statistical models to satellite-recorded remote sensing data. Even though MLR models using spectral bands gave better estimates and predictions on the field level, they could not be scaled easily to the sensor level. Therefore, for up-scaling field-developed models and for better estimation of grassland biomass, we propose using narrowband NDVI-type vegetation indices, constructed with bands in spectral regions related to canopy water content. Finally, our research has exhibited the potential and the need to link the high accuracy hyperspectral remote sensing products (e.g. biomass) with nature conservation areas like biodiversity monitoring.

Acknowledgements

The authors would like to thank the Swiss Federal Research Institute WSL and the Swiss Agency for the Environment, Forest and Landscape (SAEFL) for funding this study. Additional funding came from the 6th framework programme of the EU (contracts GOCE-CT-2007-036866 and ENV-CT-2009-226544) and the Swiss National Foundation (SNF) project HyperSwissNet. In addition, we would like to thank the anonymous reviewer for his or her valuable comments that have helped to improve the quality of the article considerably.

References

Anderson, M.C., Neale, C.M.U., Li, F., Norman, J.M., Kustas, W.P., Jayanthi, H. and Chavez, J., 2004, Up-scaling ground observations of vegetation water content, canopy height and leaf area index during SMEX02 using aircraft and Landsat imagery. *Remote Sensing of Environment*, **92**, pp. 447–464.

ASD, 2000, *FieldSpec Pro User's Guide* (Boulder, CO: Analytical Spectral Devices).

Asner, G.P., 1998, Biophysical and biochemical sources of variability in canopy reflectance. *Remote Sensing of Environment*, **64**, pp. 234–253.

Baret, F., Guyot, G. and Major, D., 1989, TSAVI: a vegetation index which minimizes soil brightness effects on LAI or APAR estimation. In *Proceedings of the 12th Canadian Symposium on Remote Sensing and IGARSS 1989*, Vancouver, Canada, pp. 1355–1358.

Barry, P., 2001, *EO-1 / Hyperion Science Data User's Guide, Level 1_B* (Redondo Beach, CA: TRW Space Defense & Information Systems).

Beeri, O., Phillips, R., Hendrickson, J., Frank, A.B. and Kronberg, S., 2007, Estimating forage quantity and quality using aerial hyperspectral imagery for northern mixed-grass prairie. *Remote Sensing of Environment*, **110**, pp. 216–225.

Bischoff, A., Auge, H. and Mahn, E., 2005, Seasonal changes in the relationship between plant species richness and community biomass in early succession. *Basic and Applied Ecology*, **6**, pp. 385–394.

Blackburn, G.A., 1998, Quantifying chlorophylls and carotenoids at leaf and canopy scales: an evaluation of some hyperspectral approaches. *Remote Sensing of Environment*, **66**, pp. 273–285.

Boschetti, M., Bocchi, S. and Brivio, P.A., 2007, Assessment of pasture production in the Italian Alps using spectrometric and remote sensing information. *Agriculture, Ecosystems and Environment*, **118**, pp. 267–272.

Broge, N.H. and Leblanc, E., 2001, Comparing prediction power and stability of broadband and hyperspectral vegetation indices for estimation of green leaf area index and canopy chlorophyll density. *Remote Sensing of Environment*, **76**, pp. 156–172.

Butterfield, H.S. and Malmstrom, C.M., 2009, The effects of phenology on indirect measures of aboveground biomass in annual grasses. *International Journal of Remote Sensing*, **30**, pp. 3133–3146.

Carter, G.A., 1994, Ratios of leaf reflectances in narrow wavebands as indicators of plant stress. *International Journal of Remote Sensing*, **15**, pp. 697–703

Carter, G.A., Knapp, A.K., Anderson, J.E., Hoch, G.A. and Smith, M.D., 2005, Indicators of plant species richness in AVIRIS spectra of a mesic grassland. *Remote Sensing of Environment*, **98**, pp. 304–316.

Cho, M.A., Skidmore, A., Corsi, F., Van Wieren, S.E. and Sobhan, I., 2007, Estimation of green grass/herb biomass from airborne hyperspectral imagery using spectral indices and partial least squares regression. *International Journal of Applied Earth Observation and Geoinformation*, **9**, pp. 414–424.

Clausen, J., 1999, *Branch and Bound Algorithms – Principles and Examples* (Copenhagen: Department of Computer Sciences, University of Copenhagen).

Clevers, J.P.G.W. and Jongschaap, R.E.E., 2001, Imaging spectrometry for agriculture. In *Imaging Spectrometry. Basic Principles and Prospective Applications*, F.D. Van der Meer and S.M. De Jong (Eds.), pp. 157–199 (Dordrecht: Kluwer Academic Publishers).

Cook, E.A., Iverson, L.R. and Graham, R.L., 1989, Estimating forest productivity with Thematic Mapper and biogeographical data. *Remote Sensing of Environment*, **28**, pp. 131–141.

Crawley, M., 2005, *Statistical Computing: An Introduction to Data Analysis using S-Plus* (Chichester: John Wiley & Sons).

Curran, P.J., 1989, Remote sensing of foliar chemistry. *Remote Sensing of Environment*, **30**, pp. 271–278.

Datt, B., Mcvicar, T.R., Van Niel, T.G., Jupp, D.L.B. and Pearlman, J.S., 2003, Preprocessing EO-1 Hyperion hyperspectral data to support the application of agricultural indexes. *IEEE Transactions on Geoscience and Remote Sensing*, **41**, pp. 1246–1259.

De Jong, S.M., Pebesma, E.J. and Lacaze, B., 2003, Aboveground biomass assessment of Mediterranean forests using airborne imaging spectrometry: the DAIS Peyne experiment. *International Journal of Remote Sensing*, **24**, pp. 1505–1520.

Dengsheng, L., 2006, The potential and challenge of remote sensing-based biomass estimation. *International Journal of Remote Sensing*, **27**, pp. 1297–1328.

Diaconis, P. and Efron, B., 1983, Computer-intensive methods in statistics. *Scientific American*, **248**, pp. 96–108.

Duelli, P. and Obrist, M.K., 2003, Regional biodiversity in an agricultural landscape: the contribution of seminatural habitat islands. *Basic and Applied Ecology*, **4**, pp. 129–138.

Eckert, S. and Kneubühler, M., 2004, Application of HYPERION data to agricultural land classification and vegetation properties estimation in Switzerland. In *Proceedings of XXth ISPRS Conference*, 12–23 July 2004, Istanbul, Turkey, (Istanbul: The International Society for Photogrammetry and Remote Sensing (ISPRS)), pp. 866–872.

Eggenberg, S., Dalang, T., Dipner, M. and Mayer, C., 2001, *Cartography and Evaluation of Dry Grassland Sites of National Importance*. Technical Report , Environmental Series 325, Nature and Landscape (Bern: Swiss Agency for the Environment Forests and Landscape (SAEFL)).

Elvidge, C.D., 1990, Visible and near infrared reflectance characteristics of dry plant materials. *International Journal of Remote Sensing*, **11**, pp. 1775–1795.

Elvidge, C.D. and Chen, Z., 1995, Comparison of broadband and narrowband red and near-infrared vegetation indices. *Remote Sensing of Environment*, **54**, pp. 38–48.

FILELLA, I. and PEÑUELAS, J., 1994, The red-edge position and shape as indicators of plant chlorophyll content, biomass and hydric status. *International Journal of Remote Sensing*, **15**, pp.1459–1470.

FILELLA, I., PEÑUELAS, J., LLORENS, L. and ESTIARTE, M., 2004, Reflectance assessment of seasonal and annual changes in biomass and CO2 uptake of a Mediterranean shrubland submitted to experimental warming and drought. *Remote Sensing of Environment*, **90**, pp. 308–318.

GEERKEN, R., BATIKHA, N., CELIS, D. and DEPAUW, E., 2005, Differentiation of rangeland vegetation and assessment of its status: field investigations and MODIS and SPOT VEGETATION data analyses. *International Journal of Remote Sensing*, **26**, pp. 4499–4526.

GONG, P., PU, R., BIGING, G.S. and LARRIEU, M.R., 2003, Estimation of forest leaf area index using vegetation indices derived from Hyperion hyperspectral data. *IEEE Transactions on Geoscience and Remote Sensing*, **41**, pp. 1355–1362.

GOULD, W., 2000, Remote sensing of vegetation, plant species richness and regional biodiversity hotspots. *Ecological Applications*, **20**, pp. 1861–1870.

HABOUDANE, D., MILLER, J.R., PATTEY, E., ZARCO-TEJADA, P.J. and STRACHAN, I., 2004, Hyperspectral vegetation indices and novel algorithms for predicting green LAI of crop canopies: modeling and validation in the context of precision agriculture. *Remote Sensing of Environment*, **90**, pp. 337–352.

HANSEN, P.M. and SCHJOERRING, J.K., 2003, Reflectance measurement of canopy biomass and nitrogen status in wheat crops using normalized difference vegetation indices and partial least squares regression. *Remote Sensing of Environment*, **86**, pp. 542–553.

HILL, T. and LEWICKI, P., 2006, *Statistics: Methods and Applications. A Comprehensive Reference for Science, Industry and Data Mining* (Tulsa: Statsoft).

HUNT, E.R., 1991, Airborne remote sensing of canopy water thickness scaled from leaf spectrometer data. *International Journal of Remote Sensing*, **12**, pp. 643–649.

JACKSON, R.D. and HEUETE, A.R., 1991, Interpreting vegetation indices. *Journal of Preventive Veterinary Medicine*, **11**, pp. 185–200.

JENSEN, J.R., 2000, *Remote Sensing of the Environment: An Earth Resource Perspective* (Upper Saddle River, NJ: Prentice-Hall).

KOGAN, F., STARK, R., GITELSON, A.A., JARGALSAIKHAN, L., DUGRAJAV, C. and TSOOJ, S., 2004, Derivation of pasture biomass in Mongolia from AVHRR-based vegetation health indices. *International Journal of Remote Sensing*, **25**, pp. 2889–2896.

KOOISTRA, L., SUAREZ BARRANCO, M.D., VAN DOBBEN, H.F. and SCHAEPMAN, M.E., 2006, Monitoring vegetation biomass in river floodplains using imaging spectroscopy. In *ISPRS 2006: ISPRS Mid-term Symposium on Remote Sensing: from Pixels to Processes*, Enschede, Netherlands. (Enschede: The International Society for Photogrammetry and Remote Sensing (ISPRS)), pp. 214–218.

KUMAR, L., SCHMIDT, K.S., DURY, S. and SKIDMORE, A.K., 2001, Imaging spectrometry and vegetation science. In *Imaging Spectrometry. Basic Principles and Prospective Applications*, F.D. Van der Meer and S.M. De Jong (Eds.), pp. 111–155 (Dordrecht: Kluwer Academic Publishers).

KÜNNEMEYER, R., SCHAARE, P.N. and HANNA, M.M., 2001, A simple reflectometer for on-farm pasture assessment. *Computers and Electronics in Agriculture*, **31**, pp. 125–136.

LIANG, S., 2004, *Quantitative Remote Sensing of Land Surfaces* (Hoboken, NJ: Wiley & Sons).

MILLER, A.J., 2002, *Subset Selection in Regression* (Boca Raton, FL: Chapman & Hall).

MIRIK, M., NORLAND, J.E., CRABTREE, R.L. and BIONDINI, M.E., 2005, Hyperspectral one-meter-resolution remote sensing in Yellowstone National Park, Wyoming: II, Biomass. *Rangeland Ecology and Management*, **58**, pp. 459–465.

MITTELBACH, G.G., STEINER, C.F., SCHEINER, S.M., GROSS, K.L., REYNOLDS, H.L., WAIDE, R.B., WILLIG, M.R., DODSON, S.I. and GOUGH, L., 2001, What is the observed relationship between species richness and productivity? *Ecology*, **82**, pp. 2381–2396.

MUTANGA, O. and SKIDMORE, A.K., 2004a, Hyperspectral band depth analysis for a better estimation of grass biomass (*Cenchrus ciliaris*) measured under controlled laboratory conditions. *International Journal of Applied Earth Observation and Geoinformation*, **5**, pp. 87–96.

MUTANGA, O. and SKIDMORE, A.K., 2004b, Narrowband vegetation indices overcome the saturation problem in biomass estimation. *International Journal of Remote Sensing*, **25**, pp. 3999–4014.

MUTANGA, O., SKIDMORE, A.K. and VAN WIEREN, S., 2003, Discriminating tropical grass (*Cenchrus ciliaris*) canopies grown under different nitrogen treatments using spectroradiometry. *ISPRS Journal of Photogrammetry and Remote Sensing*, **57**, pp. 263–272.

OINDO, B.O. and SKIDMORE, A.K., 2002, Interannual variability of NDVI and species richness in Kenya. *International Journal of Remote Sensing*, **23**, pp. 285–298.

OINDO, B.O., SKIDMORE, A.K. and DE SALVO, P., 2003, Mapping habitat and biological diversity in the Maasai Mara ecosystem. *International Journal of Remote Sensing*, **24**, pp. 1053–1069.

OSBORNE, S.L., SCHEPERS, J.S., FRANCIS, D.D. and SCHLEMMER, M.R., 2002, Use of spectral radiance to estimate in-season biomass and grain yield in nitrogen- and water stressed corn. *Crop Science*, **42**, pp. 165–171.

PALMER, M.W. and HUSSAIN, M., 1997, The unimodal (species richness–biomass) relationship in microcommunities emerging from soil seed banks. *Proceedings of the Oklahoma Academy of Science*, **77**, pp. 17–26.

PCI GEOMATICS, 2006, *OrthoEngine, User's Guide Version 10.0* (Ontario: PCI Geomatics).

PEARLMAN, J.S., BARRY, P.S., SEGAL, C.C., SHEPANSKI, J., BEISO, D. and CARMAN, S.L., 2003, Hyperion, a space-based imaging spectrometer. *IEEE Transactions on Geoscience and Remote Sensing*, **41**, pp. 1160–1173.

RAHMAN, A.F. and GAMON, J.A., 2004, Detecting biophysical properties of a semi-arid grassland and distinguishing burned from unburned areas with hyperspectral reflectance. *Journal of Arid Environments*, **58**, pp. 597–610.

RICHTER, R., 2003, *Atmospheric/Topographic Correction for Airborne Imagery*. ATCOR-4 User Guide, Version 3.0, 66 pp. DLR-IB564-02/03 (Wessling: Deutsches Zentrum für Luft- und Raumfahrt (DLR)).

ROCCHINI, D., RICOTTA, C. and CHIARUCCI, A., 2007, Using satellite imagery to assess plant species richness: the role of multispectral systems. *Applied Vegetation Science*, **10**, pp. 325–331.

SCURLOCK, J.M.O., JOHNSON, K. and OLSON, R.J., 2002, Estimating net primary productivity from grassland biomass dynamics measurements. *Global Change Biology*, **8**, pp. 736–753.

SHEN, M., TANG, Y., KLEIN, J., ZHANG, P., GU, S., SHIMONO, A. and CHEN, J., 2008, Estimation of aboveground biomass using *in situ* hyperspectral measurements in five major grassland ecosystems on the Tibetan Plateau. *Journal of Plant Ecology-UK*, **1**, pp. 247–257.

STAMPFLI, A. and ZEITER, M., 2001, Species responses to climatic variation and land-use change in grasslands of southern Switzerland. In *Biomonitoring: General and Applied Aspects on Regional and Global Scales*, C.A. Burga and A. Kratochwil (Eds.), pp. 107–124 (Dordrecht: Kluwer Academic Publishers).

STAMPFLI, A., and ZEITER, M., 2004, Plant regeneration directs changes in grassland composition after extreme drought: a 13-year study in southern Switzerland. *Journal of Ecology*, **92**, pp. 568–576.

SWISSTOPO, 2007. DHM25. Available online at: http://www.swisstopo.admin.ch/internet/swisstopo/en/home/products/height/dhm25.html (accessed 10 December 2008).

TARR, A.B., MOORE, K.J. and DIXON, P.M., 2005, Spectral reflectance as a covariate for estimating pasture productivity and composition. *Crop Science*, **45**, pp. 996–1003.

THENKABAIL, P.S., ENCLONA, E.A., ASHTON, M.S. and VAN DER MEER, B., 2004, Accuracy assessments of hyperspectral waveband performance for vegetation analysis applications. *Remote Sensing of Environment*, **91**, pp. 354–376.

THENKABAIL, P.S., SMITH, R.B. and DE PAUW, E., 2000, Hyperspectral vegetation indices and their relationships with agricultural crop characteristics. *Remote Sensing of Environment*, **71**, pp. 158–182.

TODD, S.W., HOFFER, R.M. and MILCHUNAS, G.G., 1998, Biomass estimation on grazed and ungrazed rangelands using spectral indices. *International Journal of Remote Sensing*, **19**, pp. 427–438.

TUELLER, P.T., 1998, *Vegetation Science Applications for Rangeland Analysis and Management* (Dordrecht: Kluwer Academic Publishers).

VAN DER MEER, F., DE JONG, S.M. and BAKKER, W., 2001, Analytical techniques in spectrometry. In *Imaging Spectrometry. Basic Principles and Prospective Applications*, F.D. Van der Meer and S.M. De Jong (Eds.), pp. 17–61 (Dordrecht: Kluwer Academic Publishers).

VERSTRAETE, M.M., PINTY, B. and MYNENI, R.B., 1996, Potential and limitations of information extraction on the terrestrial biosphere from satellite remote sensing. *Remote Sensing of Environment*, **58**, pp. 201–214.

WAIDE, R.B., WILLIG, M.R., STEINER, C.F., MITTELBACH, G.G., GOUGH, L., DODSON, S.I., JUDAY, G.P. and PARMENTER, R., 1999, The relationship between primary productivity and species richness. *Annual Review of Ecology and Systematics*, **30**, pp. 257–300.

WHITE, J.D., RUNNING, S.W., NEMANI, R., KEANE, R.E. and RYAN, K.C., 1997, Measurements and remote sensing of LAI in Rocky Mountain montane ecosystems. *Canadian Journal of Forest Research*, **27**, pp. 1714–1727.

WULDER, M.A., HALL, R.J., COOPS, N.C. and FRANKLIN, S.E., 2004, High Spatial Resolution Remotely Sensed Data for Ecosystem Characterization. *BioScience*, **54**, pp. 511–521.

WYLIE, B.K., MEYER, D.J., TIESZEN, L.L. and MANNEL, S., 2002, Satellite mapping of surface biophysical parameters at the biome scale over the North American grasslands: a case study. *Remote Sensing of Environment*, **79**, pp. 266–278.

XAVIER, A.C., RUDORFF, B.F.T., MOREIRA, M.A., ALVARENGA, B.S., DE FREITAS, J.G. and SALOMON, M.V., 2006, Hyperspectral field reflectance measurements to estimate wheat grain yield and plant height. *Scientia Agricola*, **63**, pp. 130–138.

ZARCO-TEJADA, P.J., USTIN, S.L. and WHITING, M.L., 2005, Temporal and spatial relationships between within-field yield variability in cotton and high-spatial hyperspectral remote sensing imagery. *Agronomy Journal*, **97**, pp. 641–653.

ZHA, Y., GAO, J., NI, S., LIU, Y., JIANG, J. and WEI, Y., 2003, A spectral reflectance-based approach to quantification of grassland cover from Landsat TM imagery. *Remote Sensing of Environment*, **87**, pp. 371–375.

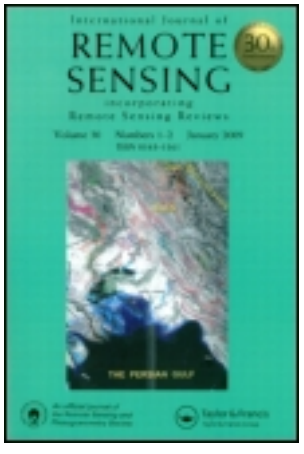

International Journal of Remote Sensing

Publication details, including instructions for authors and subscription information:
http://www.tandfonline.com/loi/tres20

Hyperspectral remote sensing for estimating aboveground biomass and for exploring species richness patterns of grassland habitats

A. Psomas [a b], M. Kneubühler [b], S. Huber [c], K. Itten [b] & N. E. Zimmermann [a]

[a] Swiss Federal Research Institute WSL, Zuercherstrasse 111, 8903, Birmensdorf, Switzerland

[b] Remote Sensing Laboratories (RSL), Department of Geography, University of Zürich, Winterthurerstrasse 190, 8057, Zürich, Switzerland

[c] Department of Geography and Geology, University of Copenhagen, Øster Voldgade 10, 1350, Copenhagen, Denmark

Available online: 18 Oct 2011

To cite this article: A. Psomas, M. Kneubühler, S. Huber, K. Itten & N. E. Zimmermann (2011): Hyperspectral remote sensing for estimating aboveground biomass and for exploring species richness patterns of grassland habitats, International Journal of Remote Sensing, 32:24, 9007-9031

To link to this article: http://dx.doi.org/10.1080/01431161.2010.532172